Çanakkale Onsekiz Mart University
Journal of Advanced Research in Natural and Applied Sciences
dergipark.org.tr/tr/pub/jarnas
Open Access

e-ISSN: 2757-5195 2024, Vol. 10, Issue 4, Pages: 954-967 doi.org/10.28979/jarnas.1562591

Accuracy of the Photometric Redshifts of Brightest Cluster Galaxies Identified in the CFHTLS-W1

Sinan Alis[1]

[1]Department of Astronomy and Space Sciences, Faculty of Science, İstanbul University, İstanbul, Türkiye

Article Info

Received: 07 Oct 2024
Accepted: 23 Dec 2024
Published: 31 Dec 2024
Research Article

Abstract— We determine the accuracy of photometric redshifts for the brightest cluster galaxies (BCGs) identified in the W1 field of the Canada-France-Hawaii Telescope Legacy Survey (CFHTLS). BCGs were identified from the galaxy cluster sample produced by the Wavelet Z Photometric (WaZP) cluster finding algorithm between $0.1 < z < 1$. Provided photometric redshifts with the CFHTLS official galaxy catalogs were compared with spectroscopic redshifts from large surveys. 101713 spectroscopic redshifts have been collected from the databases of major spectroscopic surveys. Cross-matching of 3283 BCGs with this large spectroscopic dataset yielded 1215 BCGs with high-quality spectroscopic redshift. These highly reliable spectroscopic redshifts enabled us to determine the photometric redshift accuracy of BCGs as σ_{NMAD}=0.020. The outlier fraction is obtained as 1.40%. The dispersion obtained in this study is significantly better than typical photometric redshift accuracies provided in the CFHTLS releases when all types of galaxies are included, which suggests the use of BCGs as a control object when determining galaxy cluster redshifts.

Keywords — *Photometric redshifts, brightest cluster galaxies, redshift surveys, galaxy clusters*

Subject Classification (2020)

1. Introduction

Redshift is an essential tool in extragalactic astronomy as it indicates galaxy distances. When direct distance measurements are not applicable or a large number of galaxy distances are needed, redshift can be used as an alternative measure of distance since the expansion of the Universe is imprinted in the shifts of the spectral lines of galaxy spectra.

Since the first systematic redshift surveys carried out by [1], there have been many spectroscopic redshift surveys such as Two-degree-Field Galaxy Redshift Survey (2dFGRS), Sloan Digital Sky Survey (SDSS), Very Large Telescope Visible Multi-Objects Spectrograph (VIMOS) Public Extragalactic Redshift Survey (VIPERS), Galaxy and Mass Assembly (GAMA), and Extended Baryon Oscillation Spectroscopic Survey (eBOSS). Many galaxy spectra are crucial to characterize the Universe's large-scale structure using galaxy clustering and identification of galaxy clusters. The launching of the SDSS has had an enormous impact on this regard, and thus [2] was the first to show baryonic acoustic oscillations (BAO) imprinted on the galaxy distributions due to the expansion of the Universe. The

[1]salis@istanbul.edu.tr (Corresponding Author)

discovery of the BAO signal from large-scale galaxy distributions triggered many other projects and surveys since the BAO signal is a vital tool to characterize the Universe's expansion history. The Dark Energy Spectroscopic Instrument (DESI) will obtain 35 million galaxy spectra in the next five to ten years [3]. Euclid is a space telescope designed to conduct imaging and spectroscopic surveys to obtain millions of galaxy spectra from space, specifically at the L2 point of the Earth-Sun system [4]. Nevertheless, obtaining spectra of galaxies is quite expensive in terms of telescope time, meaning longer exposure times and more extensive observational programs are required. A new era starts with large-diameter telescopes for extensive spectroscopic surveys, such as the Wide-field Spectroscopic Telescope (WST) and Mauna Kea Spectroscopic Explorer (MSE).

Another approach to overcome the need for spectroscopic redshifts is to utilize photometric redshifts. The concept of photometric redshift is based on the galaxy colors as different galaxy populations have different spectral energy distributions (i.e., SED) [5]. In this case, spectral resolution is not enough to resolve spectral lines but the overall shape of the galaxy SED.

Nowadays, all large-scale imaging surveys incorporate photometric redshift estimation in their pipelines or data products. The essential requirement for a photometric redshift estimation is imaging in multi-bands. As demonstrated in the Cosmic Evolution Survey (COSMOS), the more photometric bands, the better the accuracy of photometric redshifts [6].

In this work, we determine the accuracy of photometric redshifts of the BCGs. BCGs are giant, luminous, and hence massive early-type galaxies in the central parts of galaxy clusters. The enormous potential well at the cluster center makes BCG very special as they grow in mass and size by merging with other member galaxies of the cluster, a process known as cannibalism [7]. Using galaxy clusters detected from SDSS, [8] showed that BCGs constitute a distinct galaxy population compared to similar mass non-BCG galaxies. BCGs have steeper (~ 0.2 dex) size-luminosity relation than regular early-type galaxy populations [9]. Simulations and observational studies show that most of the stellar mass of BCGs form before $z \sim 1-2$. Thus, BCGs' recent size growth is primarily due to dry mergers taking place at the cluster centers [10–12].

We compare the photometric redshifts of our BCG sample with their spectroscopic counterparts. Determining the accuracy of photometric redshifts is crucial, as most studies rely on them. Even though accuracy is not required for large-scale studies, most galaxy evolution or galaxy population studies benefit from photometric redshifts. In this work, we aim to demonstrate the accuracy of BCGs and compare them with the ones for normal galaxies from the same survey and similar surveys.

The structure of the paper is as follows: The selection of the BCG sample, details of our photometric redshift catalog, and descriptions of spectroscopic redshift sources are given in Section 2. Section 3 compares spectroscopic redshift catalogs and cross-match photometric and spectroscopic redshifts of BCGs. The accuracy of photometric redshifts is given in Section 3.3. The conclusion of our study is given in Section 4. Throughout this paper, we use $H_0 = 70$ km s^{-1} Mpc^{-1}, $\Omega_m = 0.3$ and $\Omega_\Lambda = 0.7$.

2. Materials and Methods

In this work, we analyze the accuracy of BCG photometric redshifts using spectroscopic redshifts obtained from public surveys and databases. The present study's BCG sample is drawn from the CFHTLS. Among the four wide survey fields, we used W1, which is the largest and the one with the most extensive spectroscopic redshifts. The coordinates of the CFHTLS-W1 field are given in Table 1.

Table 1. Coordinates of the CFHTLS-W1 field

RA center	Dec center	RA(min) (deg)	Dec(min) (deg)	RA(max) (deg)	Dec(max) (deg)
02:18:00	-07:00:00	30.17771	-11.22814	38.82230	-3.70517

Center coordinates are given in sexagesimal format, whereas coordinates of the field corners are in degrees. All coordinates in the J2000 epoch.

The data used in this study were taken from the CFHTLS T0007 (final) data release [13]. CFHTLS is an imaging survey that covers about 155 deg^2 across four-wide fields (W1, W2, W3 and W4) in u*, g', r', i'/y', z' passbands. Observations were conducted using MegaCam, a mosaic camera of 36 2048×4612 pixels CCDs, with a pixel scale of 0.186". The effective field of view of the MegaCam is 0.96×0.94 deg^2. The images in five passbands have been homogeneously processed by Terapix (the former data center at the Institut d'Astrophysique Paris) to construct the final object catalogs.

In the following sections, we describe our BCG sample, the CFHTLS's photometric redshifts, and various sources of the spectroscopic redshifts.

2.1. Sample of Brightest Cluster Galaxies

The BCG sample used in this study was drawn within the framework of a TUBITAK (The Turkish Scientific and Technological Research Council) 1001 project and has been introduced in [14] and [15]. Here, we briefly describe the procedure for selecting BCGs and provide the basic properties of the sample.

Galaxy clusters in the field of CFHTLS-W1 have been identified by the cluster finder algorithm WaZP. The algorithm relies mainly on galaxy positions (RA-Dec) and photometric redshifts (zphot). Firstly, an overdensity of galaxies for a given position in the survey area is determined. The following steps analyze this position in detail by considering the different redshift slices in the line of sight. Thus, the peak of the overdensity in the redshift space is obtained. A list of cluster (overdensity) candidates is provided as an output of the pipeline. Details of the WaZP algorithm can be seen at [16, 17]. In this study, we limit ourselves to cluster candidates with a detection signal-to-noise ratio SNR > 3. This selection yields 3283 clusters in the CFHTLS-W1.

We define the BCG for each cluster based on the clustercentric distance, redshift, luminosity, and color. For a member galaxy to be defined as BCG,

i. distance to the cluster center should be less than 500 kpc,

ii. the photometric redshift of the candidate should satisfy $\mid z_{gal} - z_{cl} \mid \leq 0.03(1 + z_{cl})$

iii. the (r-i) color of the candidate should be consistent within ± 0.3 magnitudes with model elliptical galaxy colors

The choice of 500 kpc for the search radius around the cluster center is motivated by the fact that BCGs are located at the centers of galaxy clusters [7]. The cluster core (i.e., central part) is approximately 300-500 kpc around the cluster center. In [18], BCGs are identified at 300 kpc within the peak of the galaxy density distribution, while in [19], BCGs are identified within 400 kpc of the X-ray peak. Thus, we adopt the 500 kpc radius for BCG identification as also used by [20].

The brightest galaxies that satisfy the above conditions are defined as the BCG of their respective clusters. Figure 1 gives an example of a galaxy cluster used in this study and its corresponding BCG.

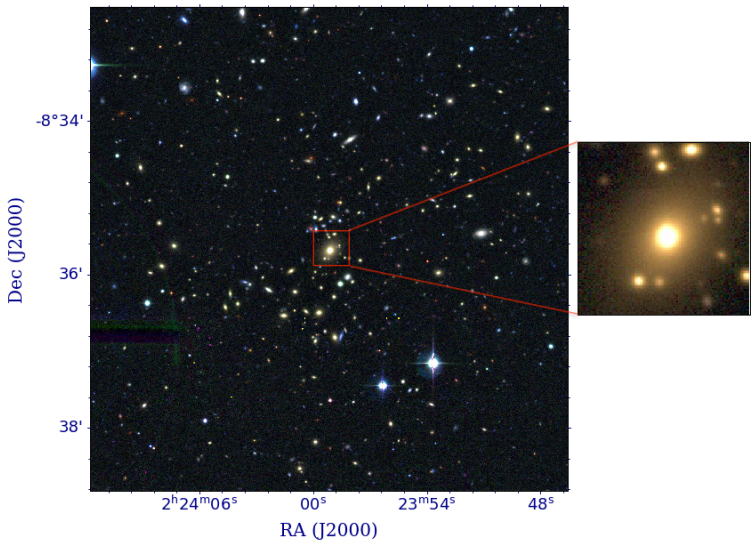

Figure 1. An example of a galaxy cluster and its BCG from our sample. The cluster shown in the image is at redshift z=0.29. The field-of-view of the central image is 1.6 Mpc, whereas the small subset on the right covers a diameter of 100 kpc

Figure 2 shows the final BCG sample's redshift distribution, and Figure 3 shows the apparent and absolute magnitude distributions.

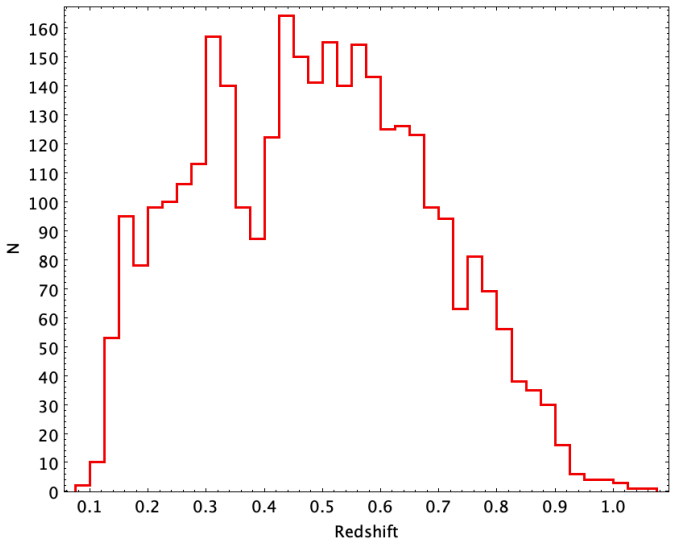

Figure 2. The redshift distribution of the BCG sample

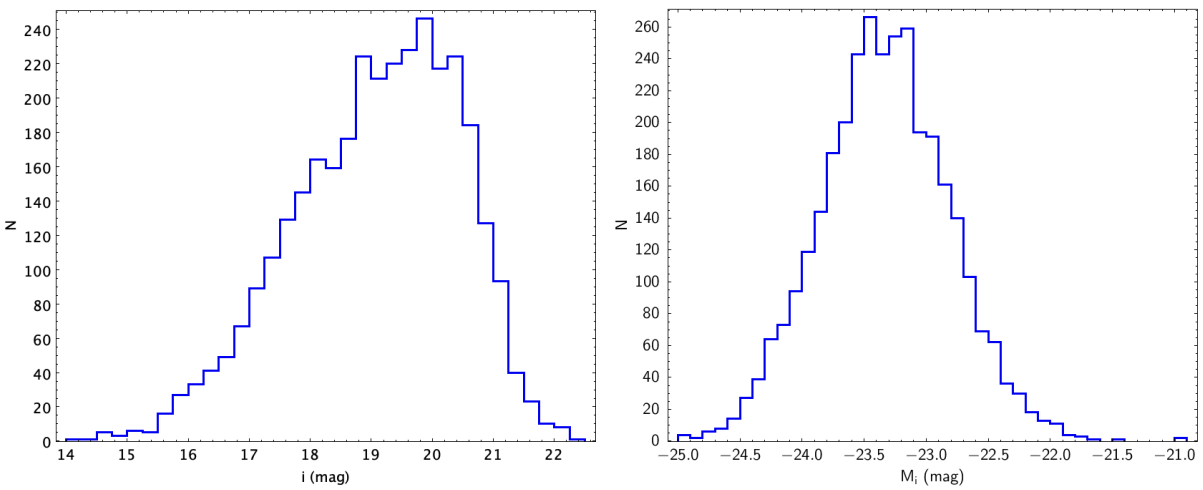

Figure 3. The i-band apparent (left) and absolute (right) magnitude distributions of the BCGs

2.2. Photometric Redshifts

In addition to object catalogs and images, Terapix also provided photometric redshifts, computed using LePhare software [21, 22]. LePhare computes the photometric redshift by fitting galaxies' spectral energy distributions (SEDs) obtained from the magnitudes in five passbands. While determining redshift, LePhare also provides a spectral type for each galaxy as a by-product. However, several spectral types are kept at a minimum to avoid color-redshift degeneracy.

Five spectral types (E, Sbc, Scd, Irr, SB) are associated with galaxies once the best match is obtained with LePhare during the SED fitting procedure. These spectral types were adopted from the observed galaxy spectra given by [23] and [24] and used similarly to [22]. Four spectra from [23] and two from [24] were extrapolated into 66 spectral templates to represent a wide range of galaxies. Photometric redshifts were computed using these final templates and explicitly optimized for CFHTLS [25] with the help of a sizeable spectroscopic sample obtained from the VIMOS Very Large Telescope Deep Survey (VVDS) [26].

2.3. Spectroscopic Redshifts

2.3.1. SDSS

SDSS is an imaging sky survey performed since 2000 with a 2.5-meter telescope in New Mexico, USA, funded by the Alfred P. Sloan Foundation. The fifth phase (SDSS-V) in the survey is being carried out. Up to now, via several observing programs, surveys have obtained spectra for more than four million galactic and extragalactic objects. The latest data release of SDSS is DR18. However, in this study, we performed a spectroscopic search within the DR17 spectroscopic catalogs [27]. The main reason is that new galaxy redshifts have not been significantly inhaled into the SDSS database since DR17, especially in the region of CFHTLS-W1. Using the CFHTLS-W1 coordinates, we used a Structured-Query Language (SQL) query and obtained spectroscopic redshifts for 14726 galaxies.

2.3.2. GAMA

GAMA survey was mainly an extragalactic survey carried out in five different fields of the celestial sky [28]. The survey was performed with the 3.9 Anglo-Australian Telescope and the AAOmega multi-object spectrograph, which can obtain spectra of nearly 400 objects simultaneously [29]. Among the GAMA observing fields, G02 is the only one overlapping with CFHTLS-W1. GAMA is a flux-limited spectroscopic survey with completeness at $r < 19.8$ in the G02 field. Similarly to SDSS, we performed a SQL search within the GAMA G02 spectroscopic catalog of the Data Release 4 to obtain spectroscopic redshifts of galaxies. This yields 36970 redshifts from the GAMA Survey.

2.3.3. VIPERS

VIPERS was a European Southern Observatory Large Program performed using one of the 8.2 m VLT telescopes and the VIMOS multi-object spectrograph [30]. VIMOS was a very efficient instrument capable of obtaining spectra of nearly 1000 objects simultaneously. VIPERS survey was conducted in the two fields of the CFHTLS, namely in W1 and W4. Since the telescope used for the VIPERS is large, the survey is designed to obtain spectra of galaxies in the redshift range of $0.5 < z < 1.1$. This makes the survey the deepest among the other redshift sources used in this study. VIPERS observed galaxies with $i < 22.5$ and published nearly 90000 spectra for galaxies in CFHTLS W1 and W4. For this study, we used the latest data release of VIPERS (PDR-2), which includes 50017 redshifts for galaxies in the CFHTLS-W1 [31].

3. Results and Discussion

3.1. Comparing Spectroscopic Catalogs

Before cross-matching photometric and spectroscopic redshifts for BCGs, we first compared the three spectroscopic redshift sources described in Section 2.3. We then carried out a pairwise comparison of spectroscopic redshifts for all three spectroscopic surveys that overlap with CFHTLS W1. Since the telescope diameters and spectrographic instruments differ, the redshift range and the number of everyday objects vary between the surveys. For this comparison, we did not restrict ourselves to BCGs but used all typical galaxies in three surveys.

Each galaxy redshift catalog is first cross-matched with another catalog, taking into account the galaxies' coordinates (i.e., right ascension and declination). As the astrometry of the respective surveys is very good, we used the matching radius to be 0.5 arcseconds. Once the match has been obtained, the spectroscopic redshift difference (Δ z) is calculated as zspec1-zspec2, where 1 and 2 denote different spectroscopic surveys. Figures 4-6 show the three pairwise spectroscopic redshift comparisons.

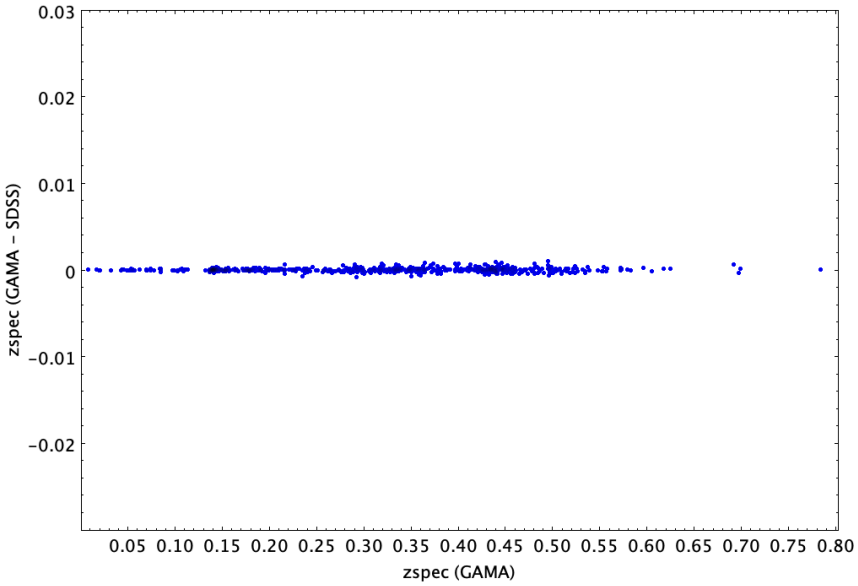

Figure 4. Spectroscopic redshift comparison between GAMA and SDSS

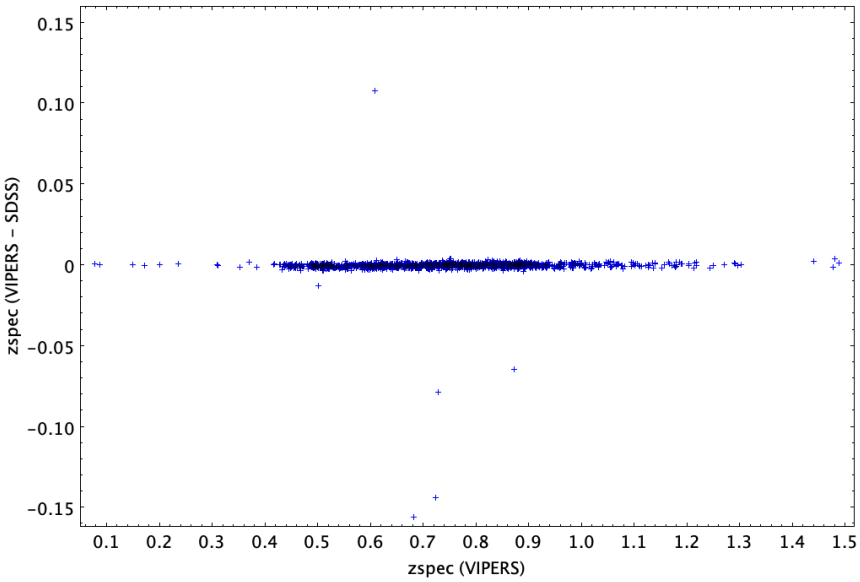

Figure 5. Spectroscopic redshift comparison between VIPERS and SDSS

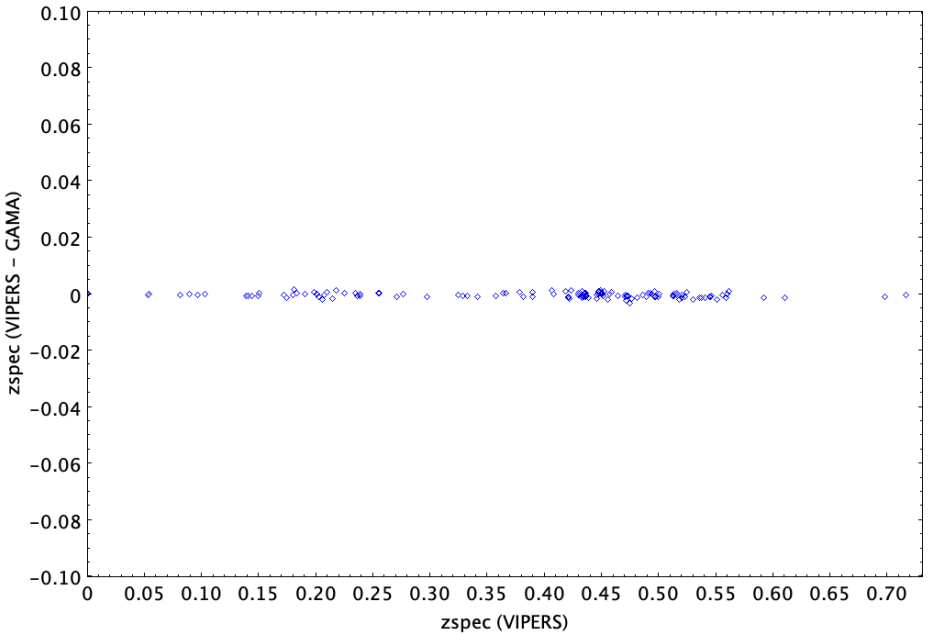

Figure 6. Spectroscopic redshift comparison between VIPERS and GAMA

The resulting comparison is summarized in Table 2. We computed the redshift difference's mean and standard deviation (Δz). Then, we eliminate galaxies with redshift differences more than three times the standard deviation (3σ). Table 2 lists the number of galaxies before and after the sigma-clipping and the resulting mean and standard deviation after the clipping has been applied. Due to sigma-clipping, 0. 9%, 0. 9%, and 6. 6% of galaxies are omitted from the comparison for SDSS-GAMA, VIPERS-SDSS, and VIPERS-GAMA, respectively. The relatively large fraction of galaxies omitted in the VIPERS-GAMA comparison comes from the fact that most of the galaxies in this comparison are at higher redshifts; hence, their redshifts can differ in different surveys. It is worth noting that VIPERS was performed with an 8m telescope, whereas GAMA was performed with a 4m telescope.

Table 2. Statistics for the pairwise survey comparison

Survey Pair	NGAL	NGAL (3σ)	$\langle\ \Delta z\ \rangle$	$\sigma(\Delta z)$
SDSS-GAMA	660	654	0.00002	0.00022
VIPERS-SDSS	1488	1474	-0.00064	0.00683
VIPERS-GAMA	151	141	-0.00054	0.00083

The first column represents survey pairs that are compared, the second column is the number of common galaxies with spectroscopic redshift, the third column is the number after outliers are removed, the fourth and fifth columns are mean difference in zspec and its standard deviation, respectively.

In all cases, the mean redshift difference between the survey pairs is much smaller than the typical error of the spectroscopic redshifts (i.e., 0.001). Therefore, all three surveys have reliable and consistent spectroscopic redshifts. Thus, combining spectroscopic redshifts from these surveys would not bring any systematic bias to our study.

3.2. Cross-Matching Photometric and Spectroscopic Redshifts

Since we wanted to assess the accuracy of photometric redshifts of BCGs, we decided to keep the most reliable spectroscopic redshifts. Thus, we apply a final filtering based on the spectra quality. Both VIPERS and GAMA surveys provide a redshift quality flag where we only keep redshifts with a confidence level of a minimum 90% for the redshift determination (zflg $\geq$ 2 for VIPERS and nQ $\geq$

3 for GAMA). For SDSS, the best approach would be to keep the high signal-to-noise spectra, where we impose a spectral quality with snMedian > 3.

A cross-matching between our BCG catalog (i.e., photometric redshifts) and the available high-quality spectroscopic redshifts reveals 94 objects from VIPERS, 447 objects from GAMA, and 682 objects from SDSS. Thus, 1223 BCGs of our sample have spectroscopic redshifts from various redshift databases. However, we did a consistency check for the matched objects and found four BCGs with multiple redshifts from VIPERS, GAMA, and SDSS. We list these BCGs in Table 3 with the corresponding redshift values. Since the listed spectroscopic redshifts in Table 3 are in good agreement and VIPERS have been conducted with an 8m telescope, we keep VIPERS redshifts for these four BCGs.

Table 3. Spectroscopic redshifts for four common BCGs from three sources

BCG ID	z (VIPERS)	z (GAMA)	z (SDSS)
5767	0.4967	0.4978	0.4961
6322	0.4553	0.4575	0.4544
7302	0.4708	0.4721	0.4815
7865	0.4299	0.4298	0.4111

After removing multiple occurrences for the BCGs mentioned above, 1215 spectroscopic redshifts are left for 1215 unique BCGs. We perform our analysis for the photometric redshift accuracy with these galaxies.

3.3. Photometric Redshift Accuracy of BCGs

The precision of the photometric redshifts is evaluated by the normalized median absolute deviation [32], which is defined as

$$\sigma_{NMAD} = 1.48\,\mathrm{median}\left(\frac{\Delta z}{1+\mathrm{zspec}}\right)$$

where Δz = |zphot - zspec|. This dispersion measure (i.e., NMAD) has been extensively used to determine photometric redshift accuracies in different galaxy surveys [6, 22, 25, 33–35]. Using spectroscopic redshifts that we obtained for 1215 BCGs and their photometric redshifts, the dispersion of the redshift accuracy was obtained as $\sigma_{NMAD} = 0.020$. In Figure 7, we compare photometric and spectroscopic redshifts for the BCG sample. The 1-σ dispersion lines are plotted around the zphot = zspec line. The scatter that we measure is due to the difference between photometric and spectroscopic redshifts. The less scatter means a better photometric redshift estimation. A better characterization of the spectral energy distribution would yield better estimates. This can be done by increasing the number of bands used to determine photometric redshifts. Table 4 compares our results with relevant imaging surveys with photometric redshift accuracies.

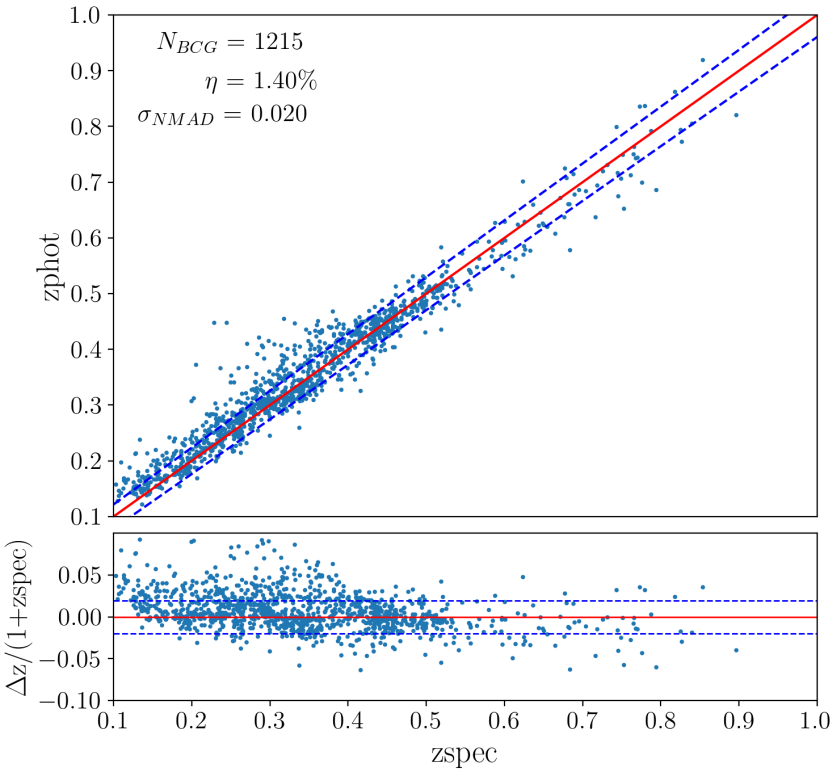

Figure 7. Comparison of photometric and spectroscopic redshifts for the 1215 BCGs. The red solid line corresponds to zphot=zspec, and the blue dashed lines show σ_{NMAD} dispersion. The bottom panel shows the $\frac{\Delta z}{1+zspec}$ residuals. The outlier fraction (η) and the 1-σ dispersion are given in the top-left side of the plot

In such studies of photometric redshift assessment, the outlier fraction is used to quantify the fraction of galaxies with large photometric and spectroscopic redshift offsets. The outlier fraction, η, (i.e., objects with catastrophic redshift errors) is computed as the fraction of galaxies with $\frac{|\Delta z|}{1+\text{zspec}} > 0.15$ [22]. There are 17 galaxies in our sample with outlier photometric redshifts according to this definition, which yields an outlier fraction of $\eta = 1.40\%$.

Table 4. Comparison of photometric redshift accuracies from the literature

Survey	NGAL	$\sigma_{\Delta z/(1+z)}$	$\eta(\%)$	Reference
CFHTLS - Deep	2867	0.029	3.80	[22]
zCOSMOS - bright	4148	0.007	0.70	[36]
CFHTLS - W1	1532	0.037	2.81	[25]
SDSS DR7 - LRG	$\sim$ 140000	0.017	0.12	[34]
Subaru HSC-SSP	$\sim$ 170000	0.066	1.99	[35]
CFHTLS - BCG	**1215**	**0.020**	**1.40**	**This Work**

Results given in the last row (i.e., bold-faced) are obtained in this study

Our results are significantly better than those of similar studies for CFHTLS, as shown in Table 4. The results of some other essential surveys are also given in the table. Among these, zCOSMOS has the most negligible dispersion (i.e., better accuracy) because the zCOSMOS survey consists of photometric data for 30 bands [6]. Including several photometric bands ensures a better characterization of the spectral energy distribution of galaxies; however, this is not the case for many imaging surveys, where five bands are used mostly.

This work presents the photometric redshift accuracy of the BCGs for the first time. Thus, it is not easy to compare directly with previous studies. Nevertheless, the survey of luminous red galaxies from the SDSS consists of the most similar galaxy sample to this work. The dispersion for $\sigma_{\frac{\Delta z}{(1+z)}} = 0.020$ obtained in this study is in good agreement with $\sigma_{\frac{\Delta z}{(1+z)}} = 0.017$ obtained with the respective SDSS sample (see Table 4). It should be noted that the much smaller outlier fraction of 0.12% obtained from SDSS is mainly the result of good spectroscopic training of the photometric redshift code used in SDSS. Many spectroscopic redshifts available in SDSS enable significantly better training for the photometric redshift code based on neural networks [37, 38].

4. Conclusion

We obtained the accuracy of photometric redshifts of the BCGs using available spectroscopic redshifts from major spectroscopic surveys. The photometric redshift accuracy of the BCGs is significantly better $\sigma_{\frac{\Delta z}{(1+z)}} = 0.020$ than that of normal galaxies in the CFHTLS. The accuracy is better, and the outlier fraction is lower than many similar galaxy samples except the zCOSMOS and the luminous red galaxy sample of SDSS. Our results can represent BCGs or luminous-red galaxies up to redshifts z$\sim$1. Since BCGs are brightest in galaxy clusters, they can easily be detected once a cluster is identified. The present study's results suggest relying on photometric redshifts of BCGs for galaxy cluster detection, especially when spectroscopic redshifts for the other cluster members are unavailable. BCGs were used to constrain cluster detection in a study based on SDSS data [39]. This study's results also suggest investigating the photometric redshift accuracy for different galaxy populations. Current (e.g., DESI, Euclid) and future large imaging surveys, such as the Large Synoptic Survey of Transients with the Rubin Observatory, will provide large galaxy catalogs. Thus, assessing the performance of photometric redshifts will be possible for different subsets of galaxies. Since BCGs are found at the center of galaxy clusters, their properties are unique. This study suggests using BCGs as control objects to constrain redshifts when determining redshifts of galaxy clusters. The photometric redshifts used in this study were obtained with LePhare, one of the most successful codes available in the literature. Incorporating machine learning techniques, especially neural networks, will probably be the primary approach in the future, as it is already being used in many surveys. However, obtaining galaxy SEDs is crucial for galaxy evolution studies; future imaging surveys with multi-bands, including optical and near-infrared, would be beneficial, increasing the photometric redshift accuracies and enabling a better SED characterization.

Author Contributions

The author read and approved the final version of the paper.

Conflicts of Interest

The author declares no conflict of interest.

Ethical Review and Approval

No approval from the Board of Ethics is required.

Acknowledgement

The brightest cluster galaxy sample of the present study was derived within the framework of the TÜBİTAK project 117F311, supported by the ARDEB-1001 program. The author acknowledges

the support and collaboration of the Extragalactic Astronomy Research Group members at Istanbul University.

References

[1] M. J. Geller, J. P. Huchra, *Mapping the universe*, Science 246 (4932) (2005) 897–903.

[2] D. J. Eisenstein, I. Zehavi, D. W. Hogg, R. Scoccimarro, M. R. Blanton, R. C. Nichol, R. Scranton, H.-J. Seo, M. Tegmark, Z. Zheng, S. F. Anderson, J. Annis, N. Bahcall, J. Brinkmann, S. Burles, F. J. Castander, A. Connolly, I. Csabai, M. Doi, M. Fukugita,..., D. G. York, *Detection of the baryon acoustic peak in the large-scale correlation function of SDSS luminous red galaxies*, The Astrophysical Journal 633 (2) (2005) 560–574.

[3] P. Martini, S. Bailey, R. W. Besuner, D. Brooks, P. Doel, J. Edelstein, D. Eisenstein, B. Flaugher, G. Gutierrez, S. E. Harris, K. Honscheid, P. Jelinsky, R. Joyce, S. Kent, M. Levi, F. Prada, C. Poppett, D. Rabinowitz, C. Rockosi, L. C. Sas,..., R. Wechsler, *Overview of the Dark Energy Spectroscopic Instrument*, in: C. J. Evans, L. Simard, H. Takami (Eds), *Ground-based and airborne instrumentation for astronomy VII*, Proceedings of the SPIE, Vol. 10702, 2018, Article ID 107021F 11 pages.

[4] Euclid Collaboration, Y. Mellier, Abdurro'uf, J. A. Acevedo Barroso, A. Achúcarro, J. Adamek, R. Adam, G. E. Addison, N. Aghanim, M. Aguena, V. Ajani, Y. Akrami, A. Al-Bahlawan, A. Alavi, I. S. Albuquerque, G. Alestas, G. Alguero, A. Allaoui, S. W. Allen, V. Allevato,..., M. Zumalacarregui, *Euclid. I. Overview of the Euclid mission*, Astronomy and Astrophysics (accepted/in press).

[5] W. A. Baum, *Photoelectric magnitudes and red-shifts*, in: George Cunliffe McVittie (Ed.), IAU Symposium on Problems of Extragalactic Research, NewYork, 1962, pp. 390–400.

[6] O. Ilbert, P. Capak, M. Salvato, H. Aussel, H. J. McCracken, D. B. Sanders, N. Scoville, J. Kartaltepe, S. Arnouts, E. Le Floc'h, B. Mobasher, Y. Taniguchi, F. Lamareille, A. Leauthaud, S. Sasaki, D. Thompson, M. Zamojski, G. Zamorani, S. Bardelli, M. Bolzonella,..., E. Zucca, *COSMOS photometric redshifts with 30-Bands for 2-deg2*, The Astrophysical Journal 690 (2) (2009) 1236–1249.

[7] J. Dubinski, *The origin of the brightest cluster galaxies*, The Astrophysical Journal 502 (1998) 141–149.

[8] A.Linden, P. N. Best, G. Kauffmann, S. D. M. White, *How special are brightest group and cluster galaxies?*, Monthly Notices of the Royal Astronomical Society 379 (2007) 867–893.

[9] M. Bernardi, J. B. Hyde, R. K. Sheth, C. J. Miller, R. C. Nichol, *The luminosities, sizes, and velocity dispersions of brightest cluster galaxies: Implications for formation history*, The Astronomical Journal 133 (2007) 1741–1755.

[10] F. S. Liu, Shude Mao, Z. G. Deng, X. Y. Xia, Z. L. Wen, *Major dry mergers in early-type brightest cluster galaxies*, Monthly Notices of the Royal Astronomical Society 396 (2009) 2003–2010.

[11] C. Lidman, G. Iacobuta, A. E. Bauer, L. F. Barrientos, P. Cerulo, W. J. Couch, L. Delaye, R. Demarco, E. Ellingson, A. J. Faloon, D. Gilbank, M. Huertas-Company, S. Mei, J. Meyers, A. Muzzin, A. Noble, J. Nantais, A. Rettura, P. Rosati,..., H. K. C. Yee, *The importance of major mergers in the build up of stellar mass in brightest cluster galaxies at $z = 1$*, Monthly Notices of the Royal Astronomical Society 433 (2013) 825–837.

[12] S. Lavoie, J. P. Willis, J. Démoclès, D. Eckert, F. Gastaldello, G. P. Smith, C. Lidman, C. Adami, F. Pacaud, M. Pierre, N. Clerc, P. Giles, M. Lieu, L. Chiappetti, B. Altieri, F. Ardila, I. Baldry, A. Bongiorno, S. Desai, A. Elyiv,..., R. J. Tuffs, *The XXL survey XV: Evidence for dry merger driven BCG growth in XXL-100-GC X-ray clusters*, Monthly Notices of the Royal Astronomical Society 462 (2016) 4141–4156.

[13] P. Hudelot, J.-Ch. Cuillandre, K. Withington, Y. Goranova, H. McCracken, F. Magnard, Y. Mellier, N. Regnault, M. Betoule, H. Aussel, J. J. Kavelaars, P. Fernique, F. Bonnarel, F. Ochsenbein, O. Ilbert, *The CFHTLS survey (T0007 release)*, 2012, Vizier Online Data Catalog p.II/317, https://cdsarc.cds.unistra.fr/viz-bin/cat/II/317.

[14] E. K. Ulgen, S. Alis, C. Benoist, F. K. Yelkenci, O. Cakir, S. Fisek, Y. Karatas, *Identification and properties of isolated field elliptical galaxies from CFHTLS-W1*, Publications of the Astronomical Society of Australia 39 (2022) Article ID e031 23 pages.

[15] E. Shaaban, S. Alis, M. Bektasoglu, F. K. Yelkenci, E. K. Ulgen, O. Cakir, S. Fisek, *Structural analysis of brightest cluster galaxies in poor and rich clusters*, New Astronomy 100 (2023) Article ID 101998 13 pages.

[16] Euclid Collaboration, R. Adam, M. Vannier, S. Maurogordato, A. Biviano, C. Adami, B. Ascaso, F. Bellagamba, C. Benoist, A. Cappi, A. Díaz-Sánchez, F. Durret, S. Farrens, A. H. Gonzalez, A. Iovino, R. Licitra, M. Maturi, S. Mei, A. Merson, E. Munari,..., G. Zamorani, *Euclid preparation. III. Galaxy cluster detection in the wide photometric survey, performance and algorithm selection*, Astronomy and Astrophysics 627 (2019) Article ID A23 27 pages.

[17] M. Aguena, C. Benoist, L. N. da Costa, R. L. C. Ogando, J. Gschwend, H. B. Sampaio-Santos, M. Lima, M. A. G. Maia, S. Allam, S. Avila, D. Bacon, E. Bertin, S. Bhargava, D. Brooks, A. Carnero Rosell, M. Carrasco Kind, J. Carretero, M. Costanzi, J. De Vicente, S. Desai,..., R. D. Wilkinson, *The WaZP galaxy cluster sample of the dark energy survey year 1*, Monthly Notices of the Royal Astronomical Society 502 (3) (2021) 4435–4456.

[18] M. Oguri, *A cluster finding algorithm based on the multi-band identification of red sequence galaxies*, Monthly Notices of the Royal Astronomical Society 444 (2014) 147–161.

[19] M. Ricci, C. Benoist, S. Maurogordato, C. Adami, L. Chiappetti, F. Gastaldello, V. Guglielmo, B. Poggianti, M. Sereno, R. Adam, S. Arnouts, A. Cappi, E. Koulouridis, F. Pacaud, M. Pierre, M. E. Ramos-Ceja, *The XXL Survey. XXVIII. Galaxy luminosity functions of the XXL-N clusters*, Astronomy and Astrophysics 620 (2018) Article ID A13 11 pages.

[20] C. J. Miller, R. C. Nichol, D. Reichart, R. H. Wechsler, A. E. Evrard, J. Annis, T. A. McKay, N. A. Bahcall, M. Bernardi, H. Boehringer, A. J. Connolly, T. Goto, A. Kniazev, D. Lamb, M. Postman, D. P. Schneider, R. K. Sheth, W. Voges, *The C4 clustering algorithm: Clusters of galaxies in the Sloan digital sky survey*, The Astronomical Journal 130 (2005) 968–1001.

[21] S. Arnouts, S. Cristiani, L. Moscardini, S. Matarrese, F. Lucchin, A. Fontana, E. Giallongo, *Measuring and modelling the redshift evolution of clustering: The hubble deep field north*, Monthly Notices of the Royal Astronomical Society 310 (2) (1999) 540–556.

[22] O. Ilbert, S. Arnouts, H. J. McCracken, M. Bolzonella, E. Bertin, O. Le Fèvre, Y. Mellier, G. Zamorani, R. Pellò, A. Iovino, L. Tresse, V. Le Brun, D. Bottini, B. Garilli, D. Maccagni, J. P. Picat, R. Scaramella, M. Scodeggio, G. Vettolani, A. Zanichelli, ..., D. Vergani, *Accurate photometric redshifts for the CFHT legacy survey calibrated using the VIMOS VLT deep survey*, Astronomy and Astrophysics 457 (3) (2006) 841–856.

[23] G. D. Coleman, C. C. Wu, D. W. Weedman, *Colors and magnitudes predicted for high redshift galaxies*, The Astrophysical Journal Supplement Series 43 (1980) 393–416.

[24] A. L. Kinney, D. Calzetti, R. C. Bohlin, K. McQuade, T. Storchi-Bergmann, H. R. Schmitt, *Template ultraviolet to near-infrared spectra of star-forming galaxies and their application to K-corrections*, The Astrophysical Journal 467 (1996) 38–60.

[25] J. Coupon, O. Ilbert, M. Kilbinger, H. J. McCracken, Y. Mellier, S. Arnouts, E. Bertin, P. Hudelot, M. Schultheis, O. Le Fèvre, V. Le Brun, L. Guzzo, S. Bardelli, E. Zucca, M. Bolzonella, B. Garilli, G. Zamorani, A. Zanichelli, L. Tresse, H. Aussel, *Photometric redshifts for the CFHTLS T0004 deep and wide fields*, Astronomy and Astrophysics 500 (3) (2009) 981–998.

[26] O. Le Fèvre, G. Vettolani, B. Garilli, L. Tresse, D. Bottini, V. Le Brun, D. Maccagni, J. P. Picat, R. Scaramella, M. Scodeggio, A. Zanichelli, C. Adami, M. Arnaboldi, S. Arnouts, S. Bardelli, M. Bolzonella, A. Cappi, S. Charlot, P. Ciliegi, T. Contini,..., D. Rizzo, *The VIMOS VLT deep survey. First epoch VVDS-deep survey: 11 564 spectra with 17.5 $\leq$ IAB $\leq$ 24 and the redshift distribution over 0 $\leq z \leq$ 5*, Astronomy and Astrophysics 439 (3) (2005) 845–862.

[27] D. S. Aguado, R. Ahumada, A. Almeida, S. F. Anderson, B. H. Andrews, B. Anguiano, E. A. Ortíz, A. Aragón-Salamanca, M. Argudo-Fernández, M. Aubert, V. Avila-Reese, C. Badenes, S. B. Rembold, K. Barger, J. Barrera-Ballesteros, D. Bates, J. Bautista, R. L. Beaton, T. C. Beers, F. Belfiore,..., H. Zou, *The fifteenth data release of the Sloan digital sky surveys: First release of MaNGA-derived quantities, data visualization tools, and stellar library*, The Astrophysical Journal Supplement Series 240 (2) (2019) Article ID 23.

[28] S. P. Driver, P. Norberg, I. K. Baldry, S. P. Bamford, A. M. Hopkins, J. Liske, J. Loveday, J. A. Peacock, D. T. Hill, L. S. Kelvin, A. S. G. Robotham, N. J. G. Cross, H. R. Parkinson, M. Prescott, C. J. Conselice, L. Dunne, S. Brough, H. Jones, R. G. Sharp, E. van Kampen,..., S. J. Warren, *GAMA: Towards a physical understanding of galaxy formation*, Astronomy and Geophysics 50 (5) (2009) 12–19.

[29] I. K. Baldry, M. Alpaslan, A. E. Bauer, J. Bland-Hawthorn, S. Brough, M. E. Cluver, S. M. Croom, L. J. M. Davies, S. P. Driver, M. L. P. Gunawardhana, B. W. Holwerda, A. M. Hopkins, L. S. Kelvin, J. Liske, Á. R. López-Sánchez, J. Loveday, P. Norberg, J. Peacock, A. S. G. Robotham, E. N. Taylor, *Galaxy And Mass Assembly (GAMA): AUTOZ spectral redshift measurements, confidence and errors*, Monthly Notices of the Royal Astronomical Society 441 (3) (2014) 2440–2451.

[30] L. Guzzo, M. Scodeggio, B. Garilli, B. R. Granett, A. Fritz, U. Abbas, C. Adami, S. Arnouts, J. Bel, M. Bolzonella, D. Bottini, E. Branchini, A. Cappi, J. Coupon, O. Cucciati, I. Davidzon, G. De Lucia, S. de la Torre, P. Franzetti, M. Fumana,..., M. Wolk, *The VIMOS public extragalactic redshift survey (VIPERS). An unprecedented view of galaxies and large-scale structure at 0.5 $< z <$ 1.2*, Astronomy and Astrophysics 566 (2014) Article ID A108 20 pages.

[31] M. Scodeggio, L. Guzzo, B. Garilli, B. R. Granett, M. Bolzonella, S. de la Torre, U. Abbas, C. Adami, S. Arnouts, D. Bottini, A. Cappi, J. Coupon, O. Cucciati, I. Davidzon, P. Franzetti, A. Fritz, A. Iovino, J. Krywult, V. Le Brun, O. Le Fèvre,..., W. J. Percival, *The VIMOS public extragalactic redshift survey (VIPERS). Full spectroscopic data and auxiliary information release (PDR-2)*, Astronomy and Astrophysics 609 (2018) Article ID A84 14 pages.

[32] D. C. Hoaglin, F. Mosteller, J. W. Tukey, *Understanding robust and exploratory data analysis*, Wiley, New York, 1983.

[33] T. Dahlen, B. Mobasher, S. M. Faber, H. C. Ferguson, G. Barro, S. L. Finkelstein, K. Finlator, A. Fontana, R. Gruetzbauch, S. Johnson, J. Pforr, M. Salvato, T. Wiklind, S. Wuyts, V. Acquaviva, M. E. Dickinson, Y. Guo, J. Huang, K.-H. Huang, J. A. Newman,..., G. Wilson, *A critical assessment of photometric redshift methods: A CANDELS investigation*, The Astrophysical Journal 775 (2) (2013) Article ID 93 26 pages.

[34] N. Greisel, S. Seitz, N. Drory, R. Bender, R. P. Saglia, J. Snigula, *Photometric redshifts and systematic variations in the spectral energy distributions of luminous red galaxies from SDSS DR7*, The Astrophysical Journal, 768 (2) (2013) Article ID 117 21 pages.

[35] M. Tanaka, J. Coupon, B.-C. Hsieh, S. Mineo, A. J. Nishizawa, J. Speagle, H. Furusawa, S. Miyazaki, H. Murayama, *Photometric redshifts for hyper suprime-cam Subaru strategic program data release 1*, Publications of the Astronomical Society of Japan 70 (SP1) (2018) Article ID S9 30 pages.

[36] S. J. Lilly, V. Le Brun, C. Maier, V. Mainieri, M. Mignoli, M. Scodeggio, G. Zamorani, M. Carollo, T. Contini, J.-P. Kneib, O. Le Fèvre, A. Renzini, S. Bardelli, M. Bolzonella, A. Bongiorno, K. Caputi, G. Coppa, O. Cucciati, S. de la Torre, L. de Ravel,..., Y. Taniguchi, *The zCOSMOS 10k-bright spectroscopic sample*, The Astrophysical Journal Supplement 184 (2) (2009) 218–229.

[37] E. Vanzella, S. Cristiani, A. Fontana, M. Nonino, S. Arnouts, E. Giallongo, A. Grazian, G. Fasano, P. Popesso, P. Saracco, S. Zaggia, *Photometric redshifts with the multilayer perceptron neural network: Application to the HDF-S and SDSS*, Astronomy and Astrophysics 423 (2004) 761–776.

[38] A. Collister, O. Lahav, C. Blake, R. Cannon, S. Croom, M. Drinkwater, A. Edge, D. Eisenstein, J. Loveday, R. Nichol, K. Pimbblet, R. de Propris, I. Roseboom, N. Ross, D. P. Schneider, T. Shanks, D. Wake, *MegaZ-LRG: A photometric redshift catalogue of one million SDSS luminous red galaxies*, Monthly Notices of the Royal Astronomical Society 375 (1) (2007) 68–76.

[39] J. Hao, T. A. McKay, B. P. Koester, E. S. Rykoff, E. Rozo, J.Annis, R. H. Wechsler, A. Evrard, S. R. Siegel, M. Becker, M. Busha, D. Gerdes, D. E. Johnston, E. Sheldon, *A GMBCG galaxy cluster catalog of 55,424 rich clusters from SDSS DR7*, The Astrophysical Journal Supplement 191 (2) (2010), 254–274.